Chapter 4

Seismic Aspects of the Application of Thermal Insulation Boards Beneath the Foundations of Buildings

David Koren, Vojko Kilar and Boris Azinović

Additional information is available at the end of the chapter

http://dx.doi.org/10.5772/62294

Abstract

In recent years, there has been a significant increase in the construction of energy-efficient buildings. These buildings are mainly characterized by their thermal envelope, which needs to follow the complete outer perimeter of the building without any interruptions, to avoid thermal bridges. It has been observed, however, that the specific new details which prevent the occurrence of thermal bridges can, in many cases, substantially affect the structural integrity of such buildings during earthquakes. This chapter deals with the seismic aspects of the application of thermal insulation (TI) boards beneath the foundations of buildings. For this purpose, the mechanical characteristics of the most commonly used material in practice (i.e., extruded polystyrene — XPS) were experimentally determined. Additionally, the shear behaviour of differently composed TI foundation sets was investigated and their friction capacity estimated. The authors have proposed a new solution for the foundation detail, which is based on controlling the sliding mechanism between the individual layers of TI boards in order to reduce the seismic forces induced on the superstructure. The proposed detail with a specially designed sliding layer surface is made of commonly used TI materials for modern passive houses, thus reducing the potential additional costs. The solution was verified by means of nonlinear dynamic analysis of several realistic building models and various friction coefficients between XPS boards. The selected results are presented in terms of fragility curves for the occurrence of sliding between the layers of XPS boards. Based on these curves, the desired seismic response scenario and level of protection of a building structure could be selected.

Keywords: thermal insulation, foundations, seismic response, energy-efficient building, extruded polystyrene (XPS), friction, sliding isolation

1. Introduction

In the European Union (EU), a large part of total energy consumption is due to the high demands for the heating/cooling of the existing building stock. It has been estimated that buildings alone cause 40% of the total energy consumption in the EU [1]. Reducing energy consumption and producing energy from renewable sources therefore represent an important research issue in the building sector. Consequently, over the last 15 years there has been an increasing trend towards the construction of energy-efficient buildings, which was also stimulated by the implementation of the directive 2010/31/EU [1]. New requirements for the energy efficiency of buildings have been set, and the year 2020 has been defined as a milestone for nearly zero-energy buildings. However, the earthquake safety of energy-efficient buildings, as well as their new construction details, needs to be investigated. In those parts of Europe where the construction of low-energy buildings has already become an established practice, earthquakes are for the most part unknown, so that such verification of new construction details is not necessary. In recent years, however, low-energy building standards [2–5] have been slowly gaining ground in areas where earthquakes (including strong earthquakes) are frequent, such as Spain, Portugal, Italy, Greece, Croatia, Slovenia and others. The suitability of the newly developed construction details for energy-efficient buildings therefore needs to be verified, and appropriate solutions found also for earthquake prone regions. This chapter emphasises on the investigation of a newly proposed structural detail which would on the one hand prevent the formation of thermal bridges, while on the other hand, it would reduce possible damage of the superstructure by acting as a seismic protection fuse during strong earthquakes.

2. Materials for thermal insulation boards

The most frequently used technique for preventing a thermal bridge occurring beneath the ground floor slab is founding of the building on thermal insulation (TI) boards, which need to have adequate compressive strength. Extruded polystyrene (XPS) boards, expanded polystyrene (EPS) boards and boards made of cellular glass are most frequently used for this purpose. They are usually placed under the reinforced concrete (RC) foundation slab or under the strip foundations in one or more layers. In order that the insulation material remains thermally functional during the whole of its expected life time, it should be resistant to long-term loadings, temperature changes (i.e., freezing/thawing cycles), creep, shrinkage and all the effects of frost, moisture and ground water. The most preferred type of boards are those whose thermal and physical characteristics do not change even if they are in constant contact with water. An example of the casting of a RC foundation slab on top of layers of XPS insulation boards is presented in **Figure 1**.

http://dx.doi.org/10.5772/62294

Figure 1. Example of extruded polystyrene (XPS) insulation boards used under a foundation slab [6].

Material property	Cellular glass	Extruded polystyrene (XPS)	Expanded polystyrene (EPS)	Polyurethane (PUR/PIR)	Mineral wool
Density ρ [kg/m^3]	100–165	25–35	15–30	30–100	40–200
Thermal conductivity λ_D [W/mK]	0.040–0.065	0.030–0.040	0.031–0.043	0.020–0.035	0.03–0.045
Water absorption W_{lp} [volume %]	<0.2	<0.3	<1.0	<1.6	<3.0
Compressive strength σ_{10} [kPa]	400–1600	100–1000	30–500	25–800	10–90
Compressive creep strength σ_{cc} [kPa]	100–700	20–300	10–150	5–250	2–30
Elastic modulus E [MPa]	100–500	15–40	5–25	2–25	0.3–2.0
Shear strength τ [kPa]	80–400	100–200	10–300	100–450	5–50
Shear modulus G [MPa]	>4.0	3.0–8.0	1.5–9.0	1.0–5.0	0.3–1.5
Energy for production* [kWh]	85	43–89	39–95	47–64	9–90
Relative material cost*	5.3–5.9	3.0–3.5	1.0–1.2	>3.0	1.0–1.5

*Energy for production and relative cost are calculated for the same thermal conductivity value of U = 0.4W/m^{2}K for both materials. The price of EPS is used as a unit [19].

Table 1. Properties of thermal insulation boards used for below-grade applications.

The most important mechanical and TI properties of commonly used TI boards, as can be found in recent catalogues and other available data in the literature [6–16], are presented in **Table 1**. The values presented in **Table 1** were obtained in monotonic static tests, whereas some of the results of cyclic tests needed for earthquake simulations are presented in Section 3. Protocols for the testing of materials and the obtaining of appropriate EU certificates are prescribed in the corresponding EU standards. For example, the presented values for compressive strengths were obtained according to the standards EN 826 [17] and EN 1606 [18], where the maximum compressive strength σ_{10} is defined at a deformation of 10%, and the long-term maximum compressive creep strength for an assumed building life-time of 50 years (σ_{cc}) is defined as the strength corresponding to a deformation of 2%.

It can be seen from **Table 1** that boards made of mineral wool have a very low compressive strength and elastic modulus, so they are presumably not suitable as TI under the foundations of a building. As well as this, mineral wool is not suitable because it can absorb more water than other materials. Polyurethane, too, appears to be unsuitable because of its lower thermal conductivity and also because the production of polyurethane is related to environmental threats to the Earth's ozone earth layer. Thus, three materials remain as being suitable for TI under foundations: XPS, EPS and cellular glass. Their microstructures are shown in **Figure 2**.

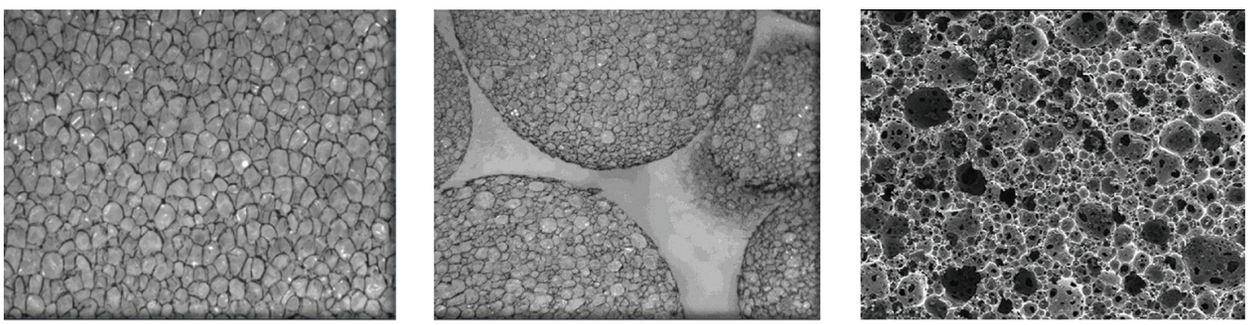

Figure 2. The microstructure of thermal insulation materials, magnified 25 times [20, 21].

XPS and EPS boards are both made from polystyrene, but their production processes (expansion or extrusion) are different. They are both formed of round-shaped grains, which are in the case of EPS polyhedral in shape and held together by process of expansion [8, 13]. The extrusion process used to produce XPS results in a more homogenous structure, which is also more repellent to water. This means that such material is more suitable in all structural details where the presence of moisture can be expected. Research into the mechanical characteristics of EPS has shown that it maintains its strength and stiffness also if it is in constant contact with water [22–24]. However, it has been shown that its thermal conductivity might increase if it is not additionally protected by a waterproofing layer. In comparison with EPS and XPS, cellular glass is more similar to XPS, since it also has a closed cell structure and is therefore highly repellent to water. Among all these three materials, EPS has the lowest strength and stiffness, but it remains interesting due to the much lower costs of its production. EPS can also be premoulded into various blocks and modules, which can replace formwork and therefore

http://dx.doi.org/10.5772/62294

significantly speed up the construction of concrete buildings. Some house manufacturers [13] allow EPS to be used under the foundation slabs of one or two storey RC/masonry houses, or even more storeys in the case of houses made of lighter materials (e.g., wood). For higher/slenderer buildings, the use of XPS or cellular glass is more appropriate. Among these, cellular glass has the best strength and stiffness characteristics, but it is much more expensive to produce and less thermally efficient. For these reasons, it is most frequently used for the insulation of multi-storey or more complex structures, where higher strength is needed.

Presently XPS is the most frequently used material for TI under foundations. It is based on the use of a polymerised polystyrol and a foaming agent. In general, rather limited research has been performed up until now into the behaviour of XPS foam, although the behaviour of this foam under monotonic compressive loading conditions is regularly controlled during the production process. In the relevant scientific literature, only a few references can be found in relation to the behaviour of XPS foam. Improved XPS foam insulation with better material efficiency (and lower thermal conductivity) was developed in [9]. An experimental study concerning the hygrothermal behaviour of retrofit solutions as applied to older stone masonry walls has, for instance, been presented in [25]. In [26] XPS foam was applied as part of a vibration isolating screen installed in soil near a test public transport track. In this research some dynamic material characteristics of the used XPS were determined by means of a white noise–forced vibration test on a freely suspended bar element: it was found that the dynamic Young's modulus of the XPS was equal to 35 MPa, whereas its density was equal to 45 kg/m^3, its Poisson's ratio to 0.2 and its material damping to 1.0%. The long-term mechanical properties (i.e., compressive creep strains and modulus), which are of key importance for TI placed under foundations, have been analysed in [27]. In the same reference, the modelling of a foundation slab resting on a TI layer has also been schematically indicated. Vaitkus et al. [28] experimentally analysed XPS short-term compression dependence on exposure time. Significant changes in the XPS strength characteristics after 45 days were observed. The relationship between the XPS foam microstructure and its response under compressive load has been analysed in [29]. The average compressive strengths of the tested samples were equal to 729, 347 and 179 kPa for the normal, transverse and longitudinal directions, respectively, and the corresponding moduli of elasticity amounted to approximately 37.0, 16.7 and 5.7 MPa. Morphological data about the XPS boards were obtained by using the X-ray tomography imaging technique and then used to develop microstructure-based finite element models. In the parametric study the effect of cell size and cell anisotropy on the mechanical response of XPS boards under compressive loads was analysed. It was shown that the microstructure cell size has no effect on the mechanical properties of XPS rigid boards when loaded in compression as long as the density of these boards remains constant. On the other hand, the degree of cell anisotropy was found to have a very important influence. Similar findings about the influence of the polymeric foam's density on mechanical properties in tension and compression have been reported in [7], where the study concludes that the foam's (e.g., XPS) deformation pattern beyond the yield point in compression is non-homogeneous. A structural macro- and microstructure analysis of XPS foam with terahertz spectroscopy and imaging was performed in [30].

As far as is known, the cyclic compressive stress–strain behaviour of XPS foam, which is essential for its seismic response in earthquake engineering applications, has not yet been researched. Furthermore, information about the cyclic behaviour of this material when subjected to shear loadings is currently a completely unresearched issue. From this point of view, extensive experimental research addressing the cyclic behaviour of XPS foam in compression, as well as in shear, has been recently performed in order to obtain a better understanding of the fundamental behaviour of this foam in earthquake engineering applications [31]. Laboratory tests were carried out on two different XPS products. These were XPS boards that were manufactured by a Slovenian enterprise and denoted as 400 L and 700 L (the number in the denotation indicates the nominal compressive strength of the XPS material in kPa). The product data are given in [6]. A servo-hydraulic testing machine was used for these tests, whereas the deformations of the XPS specimen were monitored by means of LVDTs. In the next section, the main results of the performed laboratory tests are summarized.

3. Laboratory tests

3.1. The behaviour of the XPS boards under compressive load

The compressive behaviour of the investigated XPS products was determined according to the standard SIST EN 826:1997 [17], with some modifications. The details can be found in [31]. During the performance of the monotonic compressive tests, the distance between the fixed and the movable steel plates of the testing machine was reduced until the relative deformation of the specimen reached a final value which was close to 90% (**Figure 3**). However, the compressive stress at a relative deformation of 10% was still used to estimate the XPS product's compressive strength, according to the provisions of the corresponding standard [17]. The aim of the measurements beyond a relative deformation of 10% was to determine the relative deformations of the XPS specimens, where unloading would start in the case of cyclic compressive tests. In these tests the testing procedure was similar to that used in the monotonic tests, but with additional unloading-reloading cycles at 20%, 40%, 60% and the final relative deformation of the XPS specimen.

The results of the compressive monotonic and cyclic tests are presented in **Figure 4**. The estimated compressive strengths (σ_{10}) and the compressive moduli of elasticity (E), calculated as the average of all the test results (both monotonic and cyclic), are given in **Table 2**, along with the corresponding coefficients of variation (COV). The obtained results show that the behaviour of the XPS products in compression is characterized by three regions – elastic, plastic and densification, which is typical behaviour for foamed products [28, 32–34]. The average experimentally obtained compressive strengths (σ_{10}) of the 400-L and 700-L products were 490 kPa and 752 kPa, respectively, which means that they were 22.5% and 7.4% greater than the declared compressive strength of the two products, respectively. The response of the 400-L product, which had a lower density due to the lower content of polystyrene than in the case of the 700-L product, seems to be a combination of the behaviour of elastomeric foams up to a compressive deformation of about 10%.

http://dx.doi.org/10.5772/62294

By comparing the response of the XPS products subjected to the monotonic and cyclic compressive tests, it can be seen that stress-strain envelope in the case of cyclic response corresponds to the stress-strain response obtained in the monotonic test, for both the 400-L and the 700-L products. When unloading the specimen at relative deformations of 20%, 40% and 60%, the so obtained diagram is first parallel to the elastic region, whereas later on the tangent *E*-modulus starts to decrease until a residual plastic deformation is reached at zero stress.

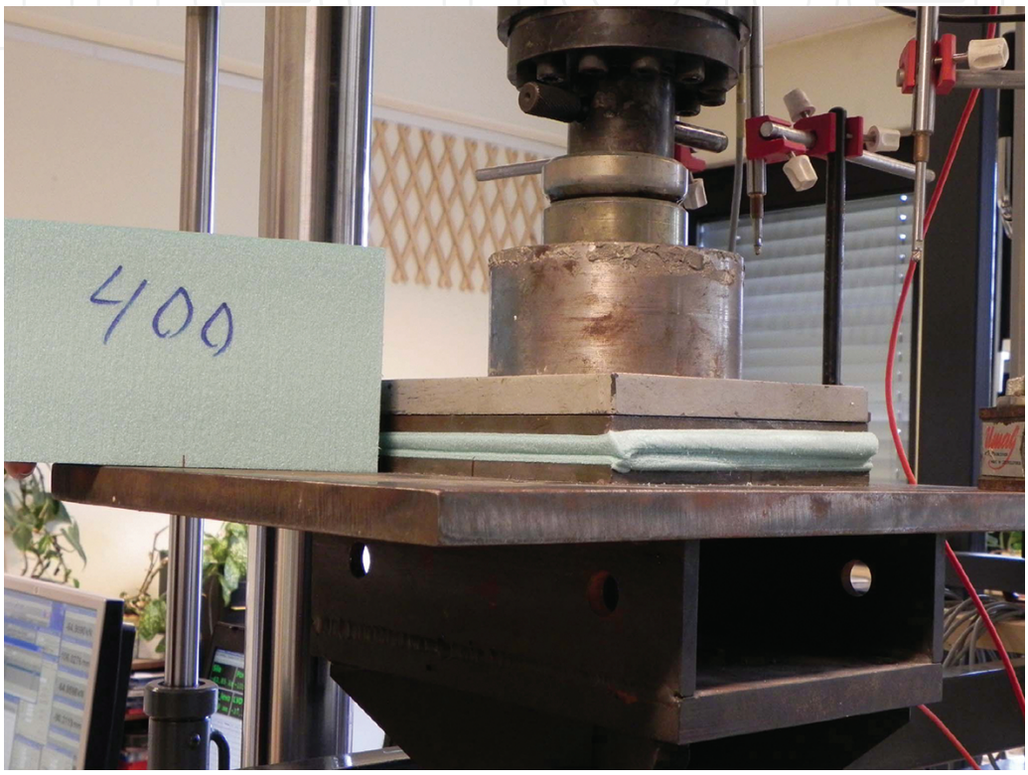

Figure 3. XPS specimen before and at the end of the compressive test.

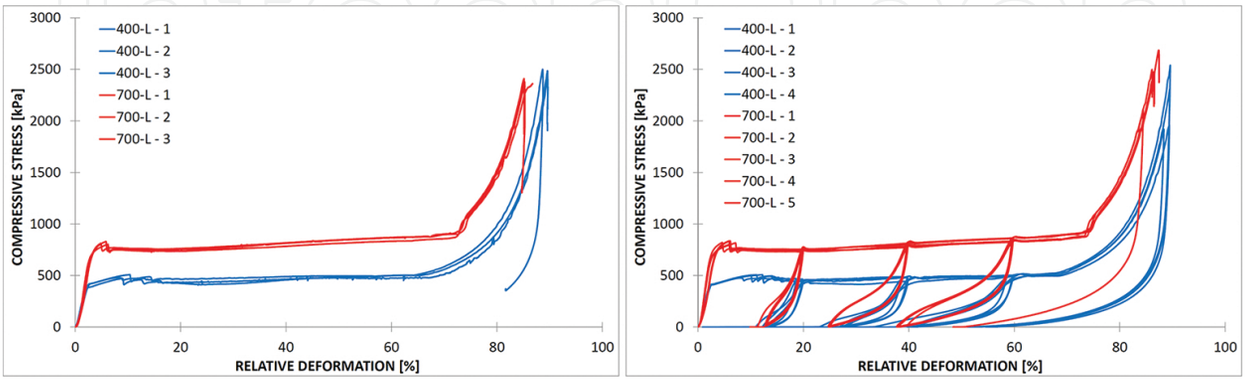

Figure 4. Compressive stress–relative deformation diagrams of the 400-L and 700-L specimens in the case of monotonic (left) and cyclic (right) compressive tests.

3.2. The behaviour of the XPS boards under shear load

The shear behaviour of the XPS products was determined according to the standard SIST EN 12090:1999 [35], using a double test specimen assembly. The test specimen consisted of two XPS blocks which were glued onto a system of three parallel steel plates where the middle plate was movable and the outer plates were fixed (**Figure 5**). The details can be found in [31]. When the monotonic shear test was carried out, the standard procedure was followed until failure of the specimen, and the shear deformation at failure was used as a reference value in order to determine the deformations where unloading of the specimen started in the case of a cyclic shear test, in which some modifications of the standard procedure were introduced. One cycle of the shear test consisted of loading until the selected deformation was reached in the "+" direction, followed by unloading to zero load, reloading until the same absolute value of deformation was obtained in the "−" direction, and then unloading to zero load. The selected deformations where unloading of the test specimen began for the cyclic tests were equal to 20%, 40%, 60%, 80% and finally 100% of the reference deformation.

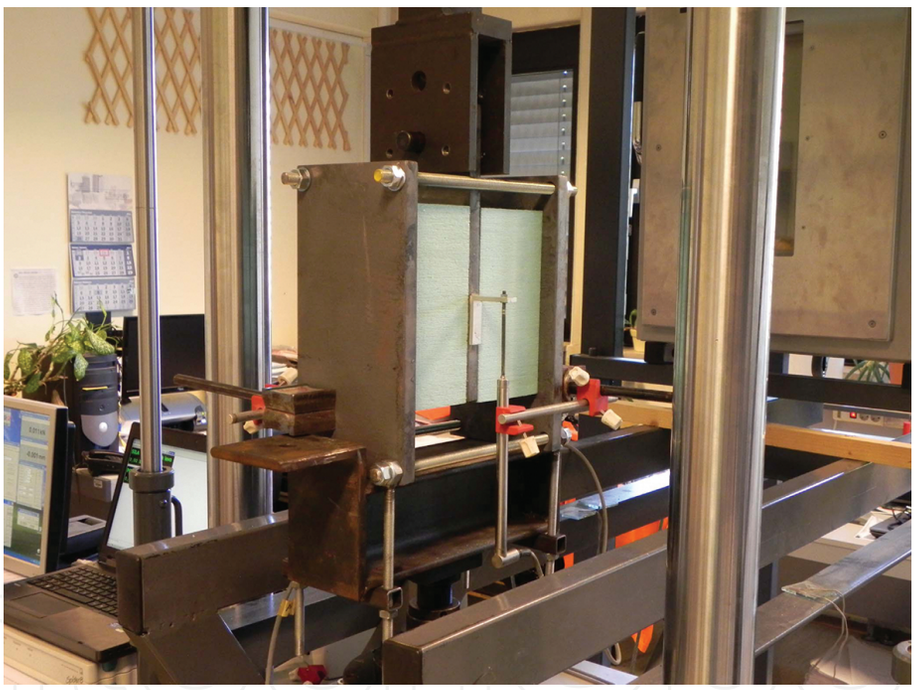

Figure 5. The XPS shear test setup.

Selected results of the shear tests are presented in **Figure 6**. The measured shear strengths (τ) and shear moduli (G), calculated as the average of all the test results (monotonic and cyclic in the "+" direction), are given in **Table 2**, together with the corresponding values of the coefficient of variation. From the results presented in **Table 2** it can be concluded that the shear strength of the 400-L and 700-L products is 3.5 times less than their corresponding compressive strength, whereas the G-modulus of the products is about 5 times less than the corresponding E-modulus. Comparing the response of the XPS in compression and in shear, it can be seen that the obtained shear ductility capacity is smaller, and that strength degradation is evident in the

http://dx.doi.org/10.5772/62294

deep nonlinear behaviour range. By comparing the response of the XPS products obtained in the monotonic and cyclic shear tests (**Figure 6**) it can be seen that the hysteresis envelope in the case of cyclic response in the "+" direction corresponds to the stress-strain response obtained in the monotonic test, for the 400-L and 700-L products. For both products the deformations corresponding to the shear failure of the foam are about the same (between 9 and 11%), but the shear strength is about 50% higher in the case of the 700-L product. Thus, the 700-L foam is able to absorb more energy in shear, too. A similar finding has been made in the case of EPS material [36]. Observing the cyclic behaviour of the 400-L and 700-L products it can be concluded that unloading at 20% of the reference deformation occurred in the elastic region, leading to zero or negligible residual plastic deformation in the tested material. When the unloading deformation was increased to 40%, 60%, 80% and 100% of the reference shear deformation, the residual plastic deformation gradually increased, too. It should also be noted that the hysteresis is not symmetric – the symmetry axis is shifted slightly into the first quadrant of the coordinate system.

	COMPRESSIVE TESTS		**SHEAR TESTS**	
Product	σ_{10} [kPa]/COV [%]	E [kPa]/COV [%]	τ [kPa]/COV [%]	G [kPa]/COV [%]
XPS400-L	490/3.5	24200/5.8	138/1.7	4520/5.1
XPS700-L	752/1.1	36100/5.3	219/5.3	7460/2.6

Table 2. Average values of the compressive strength σ_{10} and the modulus of elasticity E, and of the shear stress τ and shear modulus G.

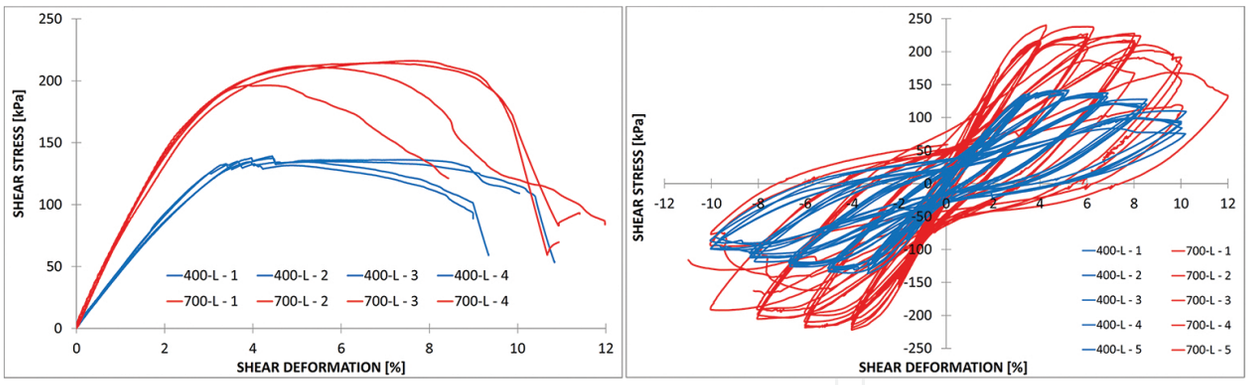

Figure 6. Shear stress–relative deformation diagrams obtained for the XPS specimens in the case of monotonic (left) and cyclic (right) shear loading tests.

3.3. Shear behaviour of the analysed TI foundation sets

In order to estimate the coefficients of friction between the different constituent elements in the TI foundation set, various shear tests were carried out. These tests have not yet been standardised and were specially developed for the needs of our experiments [31, 37]. Various TI foundation sets were analysed (**Figure 7**) – consisting of one or two XPS boards, a concrete

slab, with/without a waterproofing insulation (HI) or a polyethylene (PE) sheet. At a selected level of pre-compression (from 50 to 300 kPa) in the vertical direction of the tested set, horizontal displacements were induced by means of a servo-hydraulic actuator. The levels of pre-compression were selected based on the likely levels of compressive stress beneath the foundation slab during a moderate earthquake. For each tested TI foundation set the response and the coefficients of static (μ_s) and kinetic (μ_k) friction were determined.

Scheme of TI foundation set	Specimen ID*	Description
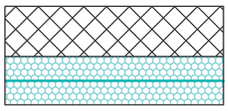	1-XPS	2 x 120 mm XPS 400-L, without a PE or HI sheet
	2-XPS	2 x 100 mm XPS 700-L, without a PE or HI sheet
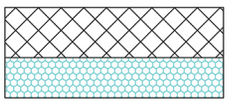	3-XPS	1 x 200 mm XPS 400-L, without a PE or HI sheet
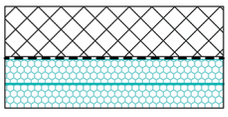	4-XPS	2 x 120 mm XPS 400-L, with a PE sheet
	5-XPS	2 x 100 mm XPS 700-L, with a PE sheet
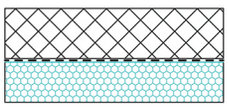	6-XPS	1 x 200 mm XPS 400-L, with a PE sheet
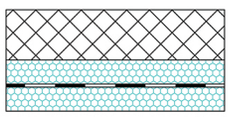	7-XPS	2 x 120 mm XPS 400-L, HI sheet without adhesive
	8-XPS	2 x 100 mm XPS 700-L, HI sheet without adhesive
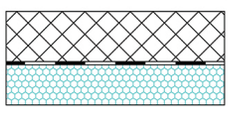	9-XPS	1 x 200 mm XPS 400-L, HI sheet without adhesive
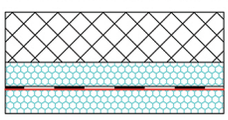	10-XPS	2 x 120 mm XPS 400-L, HI sheet having adhesive on one side only
	11-XPS	2 x 100 mm XPS 700-L, HI sheet having adhesive on one side only
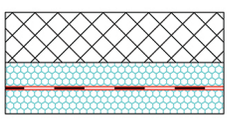	12-XPS	2 x 120 mm XPS 400-L, HI sheet having adhesive on both sides
	13-XPS	2 x 100 mm XPS 700-L, HI sheet having adhesive on both sides

* In further text and figures the test specimen's ID designation is followed by the number (50–300) representing the level of applied pre-compression level in [kPa].

Figure 7. The tested TI foundation sets.

The tests have showed that, in the case of sliding, the XPS–HI sheet contact (without adhesive on one/both sides) which was exposed to lower levels of pre-compression (e.g., 50 kPa) was the critical one. The corresponding coefficient of friction was around 0.3 [31]. In practice this means that, during a strong earthquake, it is possible that a passive house with such a foundation set would slide in the horizontal direction (**Figure 8**).

http://dx.doi.org/10.5772/62294

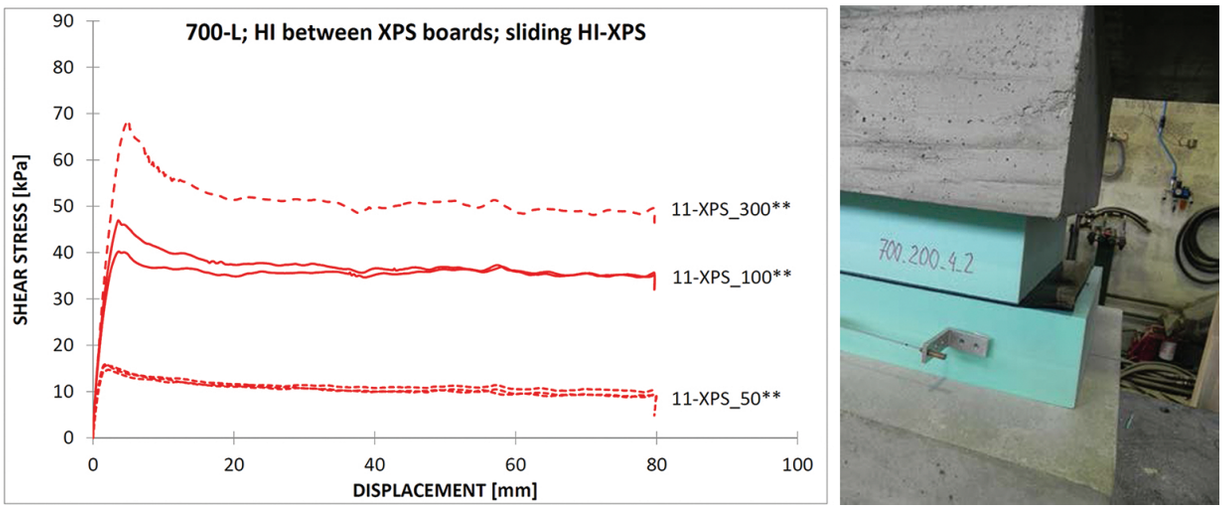

Figure 8. The 700-L TI foundation set with a HI sheet having adhesive on one side only between two XPS boards: stress–displacement diagrams at different levels of pre-compression (left) and sliding at a pre-compression level of 100 kPa (right) [31].

Another tested TI foundation sets (1-XPS and 2-XPS) consisted of two XPS boards which were in contact with the levelling concrete (without a HI or PE sheet being inserted between them). The two contact planes were carefully monitored: the XPS–XPS contact, and the XPS–levelling concrete contact. The results obtained in the tests showed that sliding occurred between the two XPS boards before sliding between the XPS and the levelling concrete. However, the test of a TI foundation set consisting of two 120 mm thick XPS boards (400-L) and levelling concrete showed a higher sliding resistance than the corresponding TI foundation set 3-XPS, which consisted of one thicker (200 mm) XPS board. The resulting coefficients of friction are presented for both TI foundation sets in **Table 3**. In the same table the obtained coefficients of friction for the TI foundation sets 4-XPS and 6-XPS are shown. These foundation sets consisted of one or two 400-L XPS boards, levelling concrete and a PE sheet inserted between them. In this case, at low pre-compression levels, sliding was observed at the contact between the PE sheet and the XPS layer or levelling concrete. At a higher pre-compression level (300 kPa) deformation of the XPS boards was observed only in the case of the two XPS boards. On the other hand, in the case of the TI foundation set with one thicker (200 mm) 400-L board (6-XPS) exposed to a pre-compression level of 300 kPa, a combination of deformation of the XPS boards and sliding between the PE sheet and the XPS was the typically observed response.

It can be concluded that TI foundation sets without a PE sheet between the levelling concrete and the XPS in general provide higher shear capacity than corresponding foundation sets with an inserted PE sheet. In the case of the TI foundation set with two 400-L boards (2 x 120 mm) this increase amounted to about 50%. The same values as those given in **Table 3** for the 2 x 120 mm 400-L boards (1-XPS, 4-XPS) can also be used in the case of the 2 x 100 mm 700-L boards (2-XPS, 5-XPS) since the μ_s values are only slightly higher in the case of the foam with a higher density.

	TI foundation set without a PE sheet between the levelling concrete and the XPS board(s)		TI foundation set with a PE sheet between the levelling concrete and the XPS board(s)	
Number and thickness of 400-L XPS boards in the TI foundation set	μ_s	μ_k	μ_s	μ_k
2 × 120 mm	0.600	0.570	0.413	0.365
1 × 200 mm	0.487	0.459	0.520	0.414

Table 3. Average values of the coefficient of maximum static (μ_s) and kinetic (μ_k) friction for the 1-XPS, 3-XPS, 4-XPS and 6-XPS foundation sets at a pre-compression level of 50 kPa.

4. A new technological solution for the foundation of passive houses in seismic areas

4.1. Description of the proposed foundation system

Recently, in [38], a new solution has been proposed with regard to the design of foundations for thermally insulated passive houses. The proposed solution is based on controlling the sliding between the individual layers of XPS boards in order to reduce the seismic forces which are induced on the superstructure. It is protected by a patent that has been filed at the Slovenian Intellectual Property Office (SIPO). The principle of the solution is analogous to that of sliding seismic base isolation systems [39–47].

The solution has been developed based on existing passive house foundation details, which were designed in order to prevent the occurrence of thermal bridges running from the heated interior of the building to the ground underneath. The proposed solution still permits the use of existing foundation construction details, while its added value consists of the additional components for the controlled response of buildings in seismically active areas, taking advantage of the sliding effect. The additional components are shown in **Figure 9** and are marked as follows; (1) vertical restrainers for the prevention of uncontrolled rocking and larger lateral shifts, (2) a lateral sliding gap (ΔH), (3) the imposed sliding surface and (4) horizontal stoppers for the prevention of sliding at the contact surface between the blinding concrete and the first layer of TI. The red arrows shown in Section A-A of **Figure 9** indicate the possible movement of the building during earthquake ground motion — if the upper part of the foundation detail shifts, together with the building, to the left, then the size of the lateral sliding gap (ΔH) on the left hand side of the building will increase and the sliding gap on the right hand side will decrease (until blocked by horizontal stoppers). In the case of very large horizontal shifts, the sliding displacement is limited by the size of the lateral sliding gap (ΔH). In this case the vertical restrainers collide with the horizontal stopper on one side of the foundation slab, whereas they separate on the opposite side until a maximum gap opening size of $2 \cdot \Delta H$ is reached. It should be mentioned that the size of the lateral sliding gap (ΔH) is defined by the buildings' designer, who can therefore limit the size of the maximum residual

http://dx.doi.org/10.5772/62294

displacement. On the other hand, the vertical restrainers prevent uncontrolled rocking of the building, as well as the occurrence of any irreversible compressive deformations of the TI layer(s). The vertical restrainers are located at defined distances around the foundation slab and are separated from one another by the distance ΔR (**Figure 9**). Vertical restrainers and horizontal stoppers can, in practice, be produced in many different ways – depending on the decision of the designer/investor and the availability/prices of the available components. It is, however, necessary, that the vertical restrainers are made of material with a high compressive strength and simultaneously a low thermal conductivity. They can consist of various hollow steel sections filled with TI, or of special pressure bearings made of thermal insulating (nano) concrete, or even of solid RC edge elements, which are additionally thermally insulated. At the contact with the soil, the vertical restrainer ends with a flat and wide surface, which prevents the negative effect of the restrainer penetrating into the soil due to the applied concentrated load (the restrainers must be placed close enough to each other — ΔR). Horizontal stoppers need to provide sufficient shear stiffness and shear strength. It is also recommended that the perimeter of the foundation base (e.g., blinding concrete) should be strengthened in order to increase the shear capacity of horizontal stoppers and to prevent protrusion of vertical restrainers.

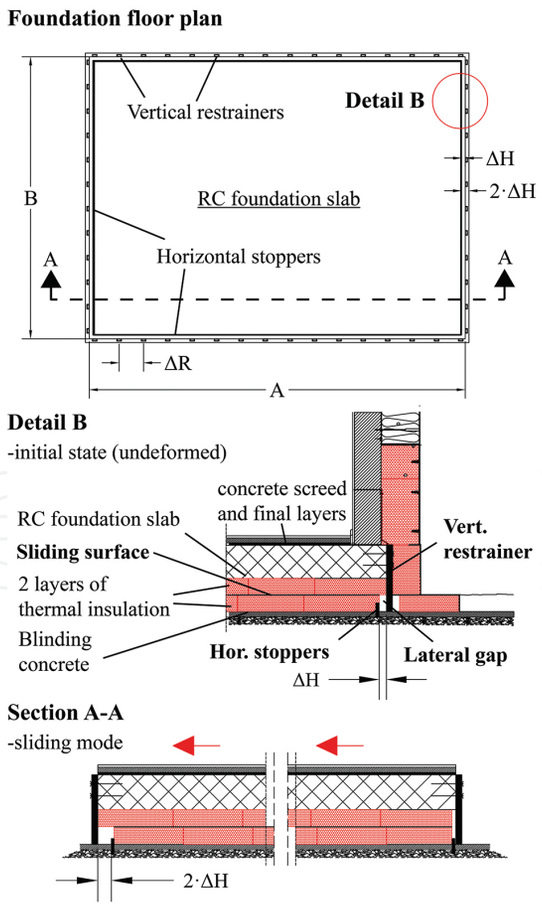

Figure 9. Section A-A and the foundation slab layout with the included anti-seismic sliding components.

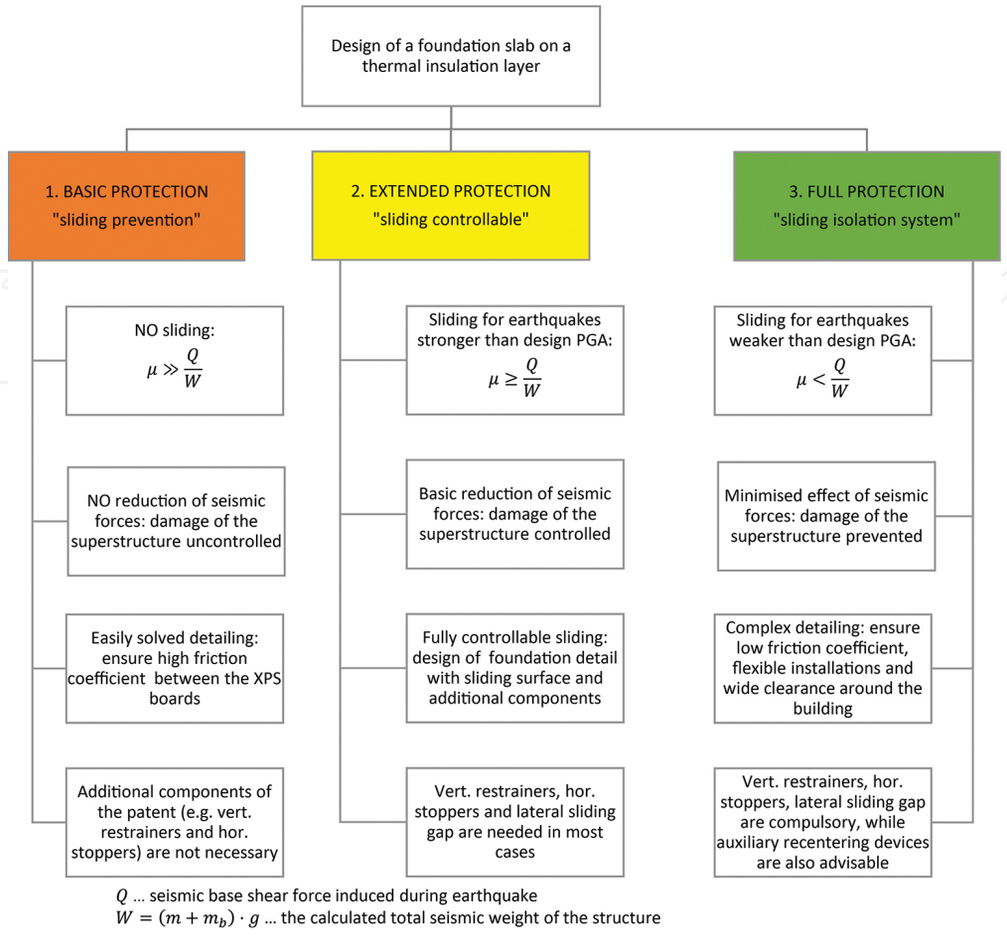

Figure 10. Overview of the characteristics of the possible seismic response scenarios.

The design of passive buildings could, according to the proposed solution, follow any of the three different seismic response scenarios that are presented in **Figure 10**. The first scenario avoids sliding and its potential benefits, but ensures basic protection of the superstructure. This concept is mainly used for simple buildings (e.g., 1–2 storey buildings), which are not vulnerable to strong seismic shaking. For such buildings the use of a sliding layer with a higher friction coefficient is advisable, since the seismic forces do not need to be reduced. In this case the application of the additional components of the proposed foundation detail (vertical restrainers, horizontal stoppers and a sliding gap) is unnecessary. The main concern, in this case, is only to ensure a sufficiently high friction coefficient between the individual layers of the foundation detail, so that the sliding mechanism is eliminated and the building's installations remain intact as in the case of conventionally founded (fixed base) buildings. For this reason, this scenario is referred to as "basic protection" (or "sliding prevention"). In the case of the second and third scenarios a reduction in the seismic forces acting on the superstructure can be achieved. The difference between the second scenario (referred to as: "extended protection" or "sliding controllable") and the third scenario (referred to as "full protection" or "sliding isolation system") depends on the seismic intensity which will activate the sliding mechanism. In the second scenario the sliding mechanism is activated only in the case of

http://dx.doi.org/10.5772/62294

earthquakes with seismic intensities higher than the design seismic intensity, whereas in the case of the third scenario sliding can also occur in the case of weaker earthquakes. The building designer and investor can therefore, together, choose the desired level of protection of the building (basic, extended, or full protection). In the case of third scenario the friction coefficient needs to have a much lower value, so that it is comparable with the friction coefficients of sliding isolators. It should be noted that, in practice, it is difficult to achieve such a low friction coefficient in the case of large areas of the foundation slab detail, so that additional costs would probably be incurred. Furthermore, in the third scenario the building designer needs to provide all of the additional components of the proposed solution which are necessary for it to be effective, i.e., flexible installations, horizontal stoppers, a lateral sliding gap (ΔH) and sufficiently wide clearance around the building. The latter is particularly important in order to avoid any pounding of an isolated structure against adjacent buildings [47].

For all of the above stated reasons the authors believe that, in the case of modern passive houses, it would be best, for the time being, to recommend the second scenario. The latter makes use of commonly available materials that have already been used in existing passive house foundation details, so that no additional costs would be incurred if a seismic fuse were to be created which would be activated only when a strong earthquake occurs.

4.2. Numerical verification and selection of the seismic response scenarios

The applicability of the proposed solution was demonstrated by means of the nonlinear dynamic analysis of some simplified parametric models, as well as of some realistic models of two, four and six storey RC passive house buildings. An extensive description of the performed analyses and the results obtained can be found in [38], whereas in this chapter only selected results are presented.

4.2.1. SDOF superstructure model

In the first stage of the study the effectiveness of the proposed solution was analysed by using a simplified Single Degree-of-Freedom (SDOF) model (**Figure 11**) which represents 2-storey (H = 6 m) passive house structures with short fundamental periods (T_{FB} = 0.10 – 0.30 s). The structures were assumed to be founded on a foundation slab (with floor plan dimensions A/B = 16/8 m) and supported by nonlinear springs in order to model the XPS boards with a nominal strength of 400 kPa and a total thickness of d = 30 cm (2 layers of thickness 15 cm). The horizontal spring for the sliding resistance of the TI foundation detail was defined based on the initial vertical compressive stresses due to the assumed mass of the superstructure during an earthquake ($m + m_b$). Six different friction coefficients (TI foundation sets) were investigated. Two different models of the superstructure were analysed, one showing elastic behaviour (with a strength factor α = 1.0 and a ductility capacity δ_c = 1.0) and the other showing nonlinear behaviour (α = 0.25 and δ_c = 4.0). The models showing elastic behaviour were investigated in order to determine the maximum response of the foundation demand parameters such as the base displacement (D_{base}), whereas the nonlinear superstructure models were used for comparison of the superstructure demand parameters, such as the ductility demand (δ_d). It should be noted that such a selection was made according to [48, 49], where it was shown that elastic

models yield maximum base engineering demand parameters (EDPs), whereas inelastic models yield maximum superstructure EDPs. The seismic response of the structural models was evaluated by means of nonlinear time-history analyses considering a set of 30 real ground motion records (GMRs), which were selected so that they matched the target spectrum for stiff soil sites (soil type A in EC8 [50]), with 5% damping and a seismic intensity of 0.25 g. Incremental dynamic analyses (IDA) were performed for each selected GMR, with a variation step of 0.02 g up to a maximum seismic intensity of 1.0 g. Uni-directional dynamic analysis was adopted, which was best suited to the available results of the uni-directional experimental tests of the XPS material [31].

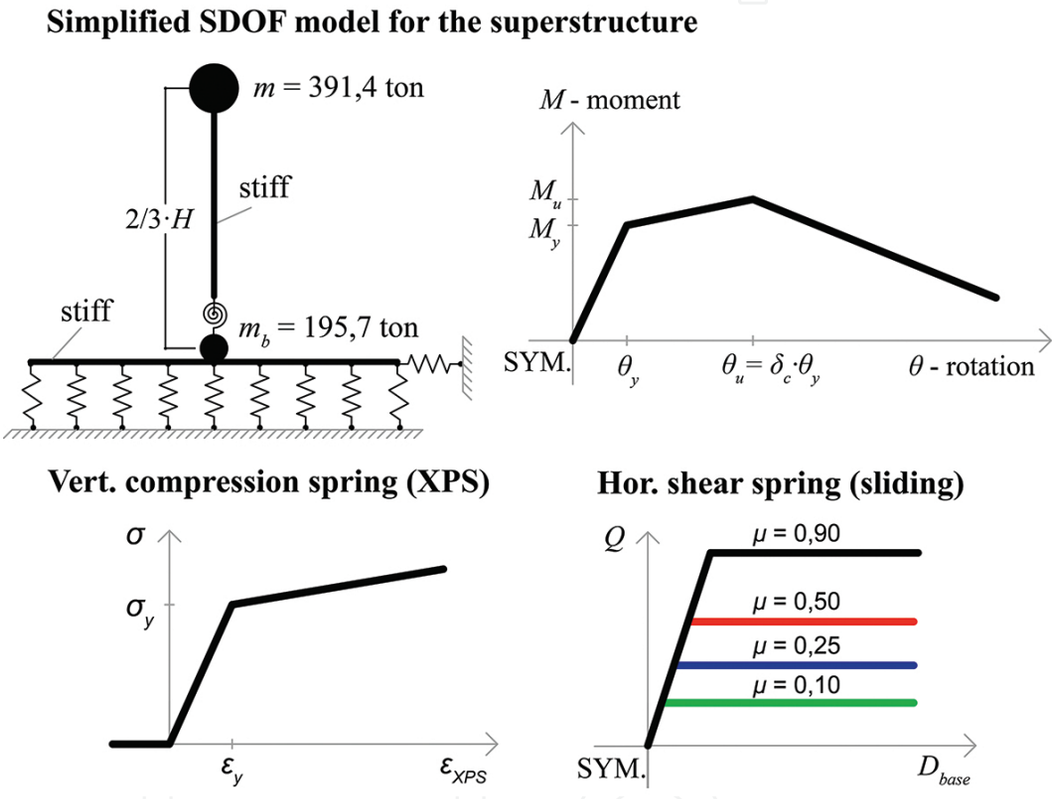

Figure 11. The numerical model considered in the parametric study.

In **Figure 12** fragility curves for the occurrence of sliding between the XPS boards are shown with the aim of illustrating the proposed seismic response scenarios. Sliding between the layers of XPS was numerically detected when the model reached the maximum resistance force of the horizontal spring (**Figure 11**). For each step of the IDA, the number of GMRs which caused sliding was calculated. The numerical probability of base sliding was then calculated as the ratio between the number of GMRs which caused sliding and the total number of analysed GMRs (30). The calculated numerical probabilities are shown in **Figure 12** in the form of stepped curves. Lognormal cumulative distribution functions were also fitted to the numerical probabilities. The fitted fragility curves were defined according to [51] and can be used to predict the seismic response scenario and to design the foundation detail accordingly.

http://dx.doi.org/10.5772/62294

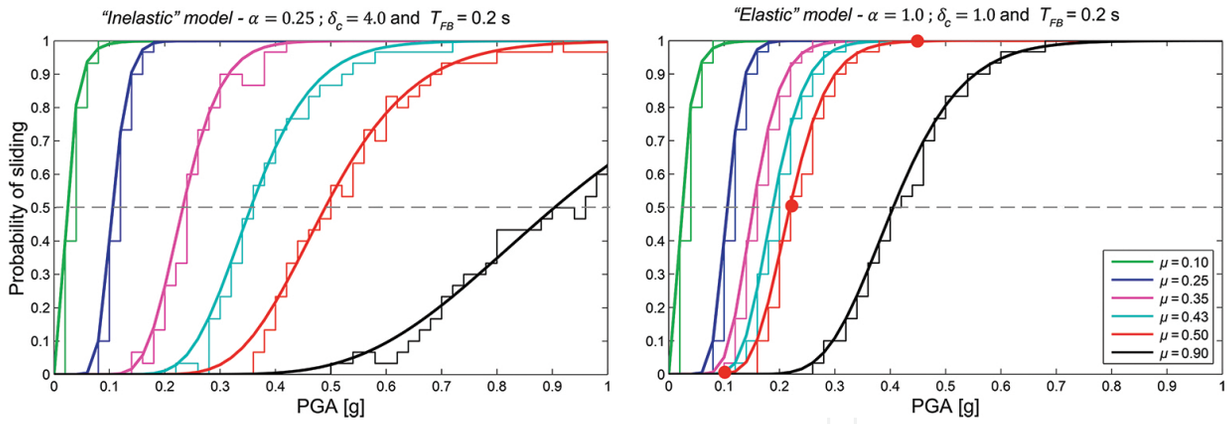

Figure 12. Fragility curves for the occurrence of sliding between the XPS boards.

Based on the presented fragility curves, an appropriate friction coefficient for the proposed foundation detail can be chosen in relation to the selected seismic response scenario. If the first seismic response scenario is selected, then the coefficients with zero probability of sliding will be the most appropriate solution for the detail. As can be seen from **Figure 12**, higher friction coefficients show zero probability of sliding for lower PGAs. On the other hand, models with lower friction coefficient values are vulnerable to sliding already at low PGAs. The third seismic response scenario, which is described as a sliding isolation system, could, on the other hand, be applied in the case of models with a 100% probability of sliding at the design PGA, whereas, for the second response scenario of controllable sliding, the use of a 50% probability of sliding at the design PGA is proposed. However, the probability of sliding for the second seismic response scenario could be selected individually by the building designer. If the desired level of protection of the superstructure is higher, the chosen probability of sliding will be closer to 100% and more similar to the third seismic response scenario. On the other hand, if the desired response at the design PGA is more similar to sliding prevention, the probability of sliding will be between 0 and 50%.

In the selected case of elastic models with μ = 0.50 the proposed seismic scenarios can be described as follows; (1) the first seismic response scenario would be allowed for PGA of less than approximately 0.10 g, (2) the second response scenario would be allowed for PGAs amounting to approximately 0.25 g and (3) the third response scenario would be required for PGAs greater than 0.45 g. It can be concluded from the above that different friction coefficients could be used for the sliding surface of the proposed foundation detail according to the selected seismic response scenario and the design PGA.

4.2.2. MDOF superstructure model

In order to verify the effectiveness of the proposed technological system in more detail, in the second stage of the study several variants of realistic multi-storey buildings were analysed. A typical passive or energy-efficient multi-storeyed RC office-building founded on a 30 cm thick RC foundation slab with a 2-layered XPS (the total thickness equal to 24 cm) beneath was used as a test example. The same building was also analysed in [52], where an evaluation of the

critical parameters which could affect the seismic behaviour of buildings founded on an XPS layer can be found. In the same reference it is also possible to access all the other modelling input data, which are not reported there. In this chapter only selected results of the characteristic (2D) frame of the analysed building are presented (**Figure 13**). In the case of the selected concrete rectangular cross-sections of the beams and columns, the minimum amount of steel reinforcement for the selected ductility class medium (DCM) according to EC8 was adopted. Soil-structure interaction (SSI) effects were taken into account by assuming that the analysed multi-storeyed frames are founded on real soils (type A according to EC8). Since, in practice, no tensile resistance is provided by the soil-structure contact, the behaviour of the soil as well as the XPS in compression was modelled by nonlinear contact springs. The behaviour of the soil in shear was modelled by means of linear elastic springs, whereas the cyclic shear behaviour of the XPS was modelled by means of a kinematic hysteresis loop with a backbone, which is presented in (**Figure 11**), taking into account a sliding gap displacement (ΔH) equal to 5 cm, and assuming that the stiffness of the third branch was equal to the initial stiffness. Seismic analyses of the investigated frame systems were carried out by means of nonlinear dynamic response analyses, which were performed by the computer program SAP2000 [53]. The vertical loads which corresponded to the seismic limit state defined in EC8 were assumed as the initial loads in all the seismic analyses, in which a group of 7 real earthquake records was applied in one (horizontal) direction. These records were scaled to three different PGA levels (0.25 g, 0.375 g and 0.50 g). Details about these nonlinear dynamic analyses can be found in [52].

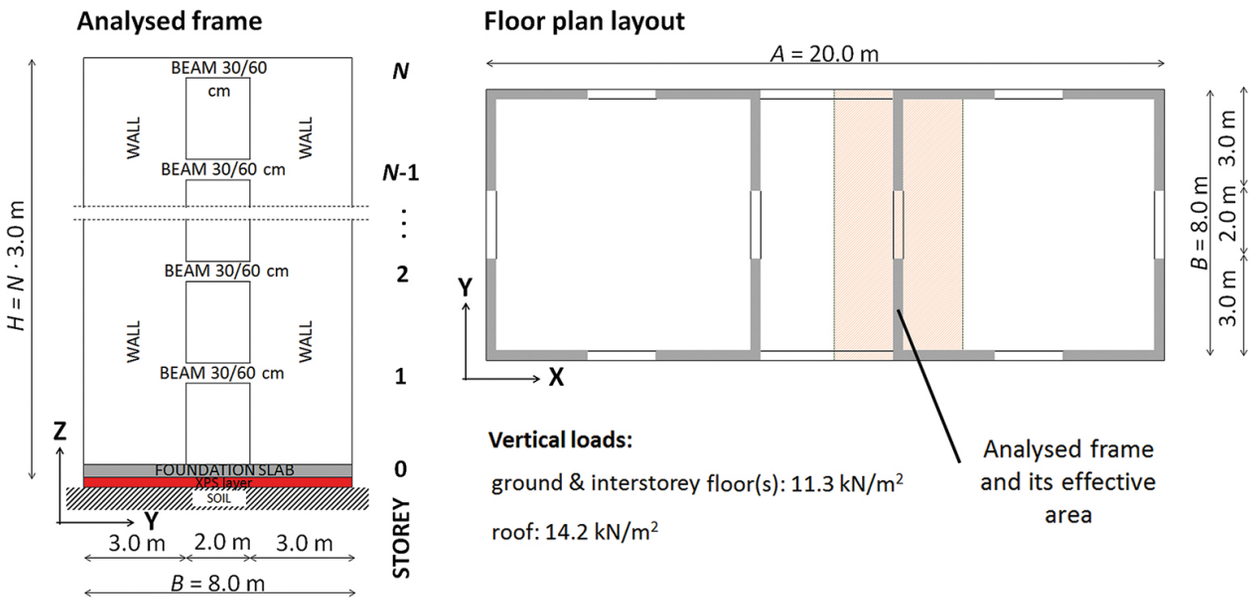

Figure 13. The investigated building's floor plan layout and the analysed 2D frame.

The seismic response of the selected analysed models which was obtained in the case of moderate seismic excitation (with a PGA equal to 1.5-times the design PGA) is presented in **Figure 14**. The typically obtained damage patterns of the 2- and 4-storeyed frames founded on

http://dx.doi.org/10.5772/62294

foundation sets with different friction coefficients (μ) are presented, together with the absolute maximum base (D_{base}) and top displacements (D_{top}) as well as the maximum compressive deformations of the XPS layer (ε_{XPS}). The damage patterns show the performance levels of the superstructure (measured with reference to the calculated rotations in the generated plastic hinges).

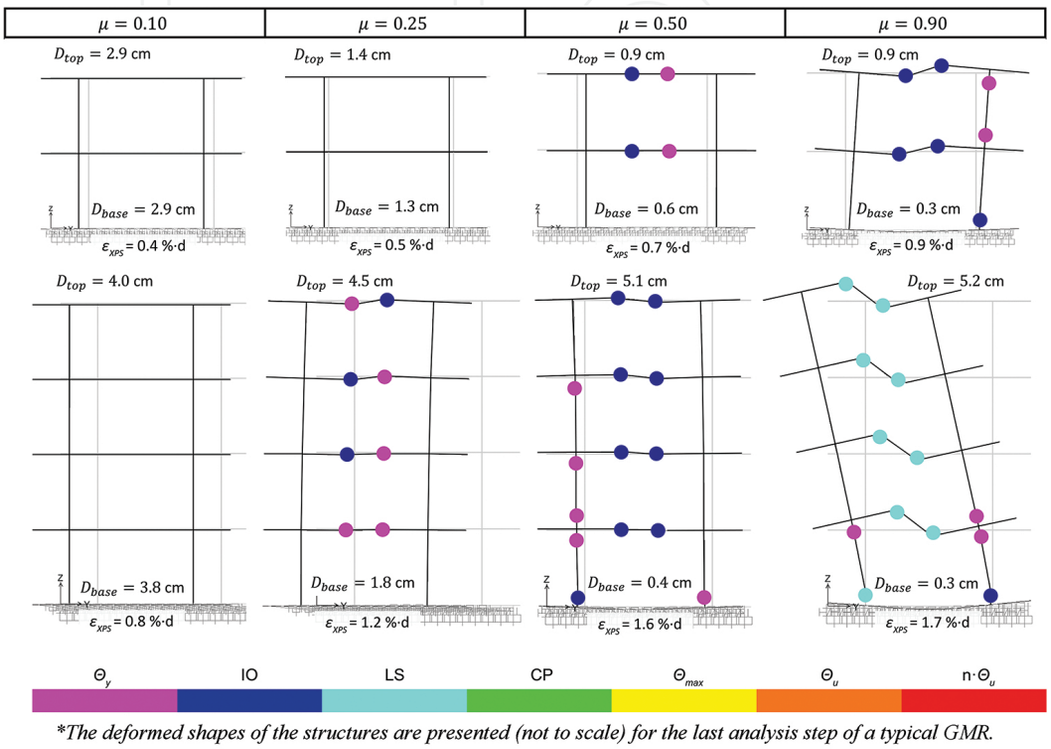

**The deformed shapes of the structures are presented (not to scale) for the last analysis step of a typical GMR.*

Figure 14. Typical damage patterns and average maximum displacements of the analysed two- and four-storeyed models subjected to PGA = 0.375 g.

It should be noted that, in all cases, the obtained base displacements (D_{base}) were smaller than the assumed gap width (ΔH = 5 cm). It can be seen that, in the case of the analysed PGA level (0.375 g), a friction coefficient of $\mu \approx 0.4$ (for 2-storeyed model) and $\mu \approx 0.2$ (for 4-storeyed model) could be used if the third seismic response scenario (i.e., a sliding isolation system) were to be selected. In the case of higher values of the friction coefficient, the second (i.e., sliding controllable) or first (i.e., sliding prevention) seismic response scenario could be expected. In this connection, the limited damage state (i.e., with plastic hinges generated in the beams only) can be interpreted as acceptable for the second seismic scenario. In the analysed case the second scenario was reached when a friction coefficient of up to approximately μ = 0.5 (for the 2-storeyed model), or approx. μ = 0.25 (for the 4-storeyed model), was selected, whereas the first scenario occurred in the case of the higher friction coefficient values ($\mu \approx 0.9$ and $\mu \approx 0.35$ for the 2- and 4-storeyed models, respectively). It should be mentioned that, in the case of 4-storeyed model subjected to the design PGA level (0.25 g), the first (second) scenario occurred when a friction coefficient equal to approximately μ = 0.5 (0.3) was selected, whereas the 2-storeyed models remained within the elastic range at the design PGA 0.25 g for all the

considered values of μ. Furthermore, it should be noted that the response of slender frames with large height-to-width ratios (e.g., the analysed 6-storeyed frame, which – for the sake of brevity – is not shown) is governed strongly by the rocking mode of oscillation, which is evident from the obtained maximum edge compressive deformations of the XPS (ε_{XPS}). As can be observed also from the results presented in **Figure 14**, the sliding isolation system successfully protects the superstructure against a rocking mechanism, since, in the case of the 4-storeyed frame, ε_{XPS} decreases from 1.7% (sliding prevention) to 0.8% (sliding isolation system).

5. Conclusions

To successfully thermally insulate a building's foundations, a TI material with sufficient TI characteristics, compressive strength, water resistance, minimal long-term creep and good durability has to be used. In this chapter, the TI materials which are most commonly used beneath foundations (i.e., XPS, EPS, cellular glass, polyurethane and mineral wool) are presented, together with their basic mechanical properties. It can be seen that boards made of mineral wool have very low strength, stiffness and water resistance, so they are unsuitable to be used for this purpose. Boards made of polyurethane can also be deemed to be unsuitable because the production of this material can have negative effects on the Earth's ozone layer. Thus, three materials remain as being suitable for TI layers under foundations: XPS, EPS and cellular glass foam. Among them, at present boards made of XPS foam are the most commonly used due to their high water resistance, relatively high strength and competitive price.

The mechanical characteristics of XPS foam boards, which need to be known for the seismic analysis of buildings founded on XPS boards, were determined by means of laboratory tests. The results showed their measured compressive strength is, in general, always greater than the declared value, which defines the nominal class of the XPS. On the other hand, the obtained values of the elastic moduli are, as a rule, slightly lower than the declared values, which can be found in the producers' catalogues. The compressive and shear behaviour of XPS under monotonic and cyclic loading conditions has shown to have a very stable response, which is true for all the investigated test specimens. In general, the capacity to absorb energy in compression as well in shear is higher in the case of XPS material with a higher declared compressive strength. The values of the measured shear characteristics, which up to now have not been provided by the producers, were as follows: 0.14 (0.22) MPa (strength) and 4.5 (7.5) MPa (modulus) for XPS 400-L (700-L).

Besides its behaviour under monotonic and cyclic compressive as well as shear loading conditions, the sliding behaviour of differently composed TI foundation sets at different pre-compression levels was also investigated and their friction capacity estimated. Based on the results of an extensive parametric study of the seismic response of buildings [48], it was found that sliding between the individual components of TI foundation sets is a likely failure mechanism in the case of low-rise, light-weight and slender buildings subjected to seismic loads. The TI foundation set consisting of two XPS boards and a waterproofing layer (HI) in between (having adhesive on one side only) showed the smallest frictional capacity (the

http://dx.doi.org/10.5772/62294

corresponding coefficient of friction at a pre-compression level of 50 kPa was around 0.3). It can be concluded that, in the case of TI foundation sets consisting of two XPS boards without a HI or PE sheet between them, the coefficient of friction amounted to 0.6, whereas coefficient of friction around 0.5 was obtained in tests of the contact between the XPS and the concrete. It was shown that the quality of the XPS boards (400 L and 700 L) did not significantly affect the frictional capacity of the analysed TI foundation set.

The results obtained in the performed numerical study of typical passive buildings have shown that foundation details, which permit sliding between the layers of TI boards by using low friction contact surfaces, can significantly reduce or even eliminate damage to the superstructure and thus act as a seismic fuse. The proposed seismic response scenarios (referred to as "sliding prevention", "sliding controllable" and the "implementation of a sliding isolation system") were demonstrated by means of nonlinear dynamic analysis for selected RC passive house structures with two and four storeys. Based on the fragility curves obtained by IDA for the occurrence of sliding between the layers of XPS boards, the likely seismic response scenario can be estimated depending on the PGA and the available friction coefficient. It is shown that lower values of the friction coefficient between the layers of TI boards reduce the level of damage to the superstructure. However, in this scenario large base displacements can occur, which must be taken into account when designing the size of the gap clearance, to prevent unfavourable pounding effects.

Based on all of the results obtained, it seems that the best solution is the implementation of a "sliding isolation system scenario", which works in a similar way to base isolation systems, and can provide full protection of the superstructure. However, from the financial point of view, this scenario usually requires some additional direct and hidden costs, which are frequently difficult for future owners to accept. To achieve this scenario more elaborate low friction material needs to be used, as well as more refined flexible installation systems, which could influence the final price of the newly built energy-efficient building. In the authors' opinion, at present the most feasible solution seems to be the "sliding controllable scenario", in which only easily available materials are needed. Such materials are already required under the foundations of modern energy-efficient buildings in order to prevent thermal bridges (they are governed by modern guides for low energy consumption). Thus, in this case the additional costs for horizontal stoppers and vertical restrainers (if required) would be low, as well as the costs of waterproofing (foil) materials with suitable low friction coefficients, which are in any case needed for all energy-efficient buildings, where they act as a waterproofing layer or a hydraulic barrier. The sliding controllable scenario can therefore be achieved without any significant additional financial costs and is therefore appropriate for use, on a wide scale, in the design of new energy-efficient buildings in earthquake-prone areas.

Acknowledgements

The financial support of the Slovenian Research Agency (Program No. P5-0068) is hereby gratefully acknowledged.

Author details

David Koren, Vojko Kilar and Boris Azinović*

*Address all correspondence to: boris.azinovic@fa.uni-lj.si

University of Ljubljana, Faculty of Architecture, Ljubljana, Slovenia

References

[1] European parliament and council. Directive 2010/31/EU of the European parliament on the energy performance of buildings. Brussels, 2010.

[2] Feist W. Wärmebrücken und Tragwerksplanung—die Grenzen des Wärmebrücken-freien Konstruirens. Darmstadt: Passivhaus Institut; 2007. 147 p.

[3] Dequaire X. Passivhaus as a low-energy building standard: contribution to a typology. Energy Efficiency. 2012;5(3):377–391. DOI: 10.1007/s12053-011-9140-8

[4] Praznik M, Butala V, Zbašnik Senegačnik M. Simplified evaluation method for energy efficiency in single-family houses using key quality parameters. Energy and Buildings. 2013;67:489–499. DOI: 10.1016/j.enbuild.2013.08.045

[5] Proietti S, Sdringola P, Desideri U, Zepparelli F, Masciarelli F, Castellani F. Life Cycle Assessment of a passive house in a seismic temperate zone. Energy and Buildings. 2013;64:463–472. DOI: 10.1016/j.enbuild.2013.05.013

[6] FIBRAN. Extruded polystyrene thermal insulation FIBRANxps [Internet]. 2015. Available from: http://www.fibran.com/files4users/files/documentation%20XPS/100_%5BEN_%5DLowRes.pdf [Accessed: 2015-12-5]

[7] Ramsteiner F, Fell N, Forster S. Testing the deformation behaviour of polymer foams. Polymer Testing. 2001;20(6):661–670. DOI: 10.1016/S0142-9418(00)00090-8

[8] Papadopoulos AM. State of the art in thermal insulation materials and aims for future developments. Energy and Buildings. 2005;37(1):77–86. DOI: 10.1016/j.enbuild.2004.05.006

[9] Bunge F, Merkel H. Development, testing and application of extruded polystyrene foam (XPS) insulation with improved thermal properties. Bauphysik. 2011;33(1):67–72. DOI: 10.1002/bapi.201110008

[10] Gnip IY, Vaitkus S, Keršulis V, Vėjelis S. Analytical description of the creep of expanded polystyrene (EPS) under long-term compressive loading. Polymer Testing. 2011;30(5):493–500. DOI: 10.1016/j.polymertesting.2011.03.012

[11] ROCKWOOL. Thermal insulation slab Rockwool [Internet]. 2015. Available from: http://www.rockwool.co.uk/products/u/2014.construction/11318/floors/ground-floors [Accessed: 2015-12-3]

[12] FOAMGLAS. Technische Daten FOAMGLAS Platten [Internet]. 2015. Available from: http://de.foamglas.com/de/waermedaemmung/produkte/produktuebersicht/foam-glas_platten/ [Accessed: 2015-12-12]

[13] JUBHome. Instructions for design of JUBhome base [Internet]. 2015. Available from: http://www.jub.si/jubhome-hise/nasveti/navodila-za-projektiranje-jubhome-base [Accessed: 2015-12-5]

[14] ELFOAM. Technical data ELFOAM boards [Internet]. 2015. Available from: http://www.elliottfoam.com/tech.html [Accessed: 2015-5-12]

[15] Diascorn N, Calas S, Sallée H, Achard P, Rigacci A. Polyurethane aerogels synthesis for thermal insulation—textural, thermal and mechanical properties. The Journal of Supercritical Fluids. 2015;106:76–84. DOI: 10.1016/j.supflu.2015.05.012

[16] Lyons A. Materials for architects and builders. London: Routledge; 2014. 512 p.

[17] CEN. European standard EN 826:2013: Thermal insulating products for building applications—Determination of compression behaviour. Brussels, 2013.

[18] CEN. European standard EN 1606:2013: Thermal insulating products for building applications—Determination of compressive creep. Brussels, 2013.

[19] ZRMK, AURE. Thermal insulating materials - thermal insulation of buildings [Internet]. 2003. Available from: http://www.aure.gov.si/eknjiznica/IL_2-03.PDF [Accessed: 2015-15-5]

[20] XPSA. Polystyrene based insulation boards products comparison [Internet]. 2015. Available from: http://www.xpsa.com/tech-info.html [Accessed: 2015-12-5]

[21] Méar F, Yot P, Viennois R, Ribes M. Mechanical behaviour and thermal and electrical properties of foam glass. Ceramics International. 2007;33(4):543–550. DOI: 10.1016/j.ceramint.2005.11.002

[22] Athanasopoulos GA, Pelekis PC, Xenaki VC. Dynamic properties of EPS geofoam: An experimental investigation. Geosynthetics International. 1999;6(3):171–194.

[23] Ossa A, Romo MP. Dynamic characterization of EPS geofoam. Geotextiles and Geomembranes. 2011;29(1):40–50. DOI: 10.1016/j.geotexmem.2010.06.007

[24] Trandafir AC, Bartlett SF, Lingwall BN. Behavior of EPS geofoam in stress-controlled cyclic uniaxial tests. Geotextiles and Geomembranes. 2010;28(6):514–524. DOI: 10.1016/j.geotexmem.2010.01.002

[25] Tomažič S, Logar V, Kristl Ž, Krainer A, Škrjanc I, Košir M. Indoor-environment simulator for control design purposes. Building and Environment. 2013;70:60–72. DOI: 10.1016/j.buildenv.2013.08.026

[26] François S, Schevenels M, Thyssen B, Borgions J, Degrande G. Design and efficiency of a composite vibration isolating screen in soil. Soil Dynamics and Earthquake Engineering. 2012;39:113–127. DOI: 10.1016/j.soildyn.2012.03.007

[27] Merkel H. Determination of long-term mechanical properties for thermal insulation under foundations. Buildings conference IX; USA, Atlanta: ASHRAE; 2004. p. 7.

[28] Vaitkus S, Vejelis S, Kairyte A. Analysis of extruded polystyrene short-term compression dependence on exposure time. Medziagotyra. 2013;19(4):471–474. DOI: 10.5755/j01.ms.19.4.2582

[29] Sadek E, Fouad N. Finite element modeling of compression behavior of extruded polystyrene foam using X-ray tomography. Journal of Cellular Plastics. 2013;49(2):161–191. DOI: 10.1177/0021955x13477436

[30] Abina A, Puc U, Jeglič A, Zidanšek A. Structural analysis of insulating polymer foams with terahertz spectroscopy and imaging. Polymer Testing. 2013;32(4):739–747. DOI: 10.1016/j.polymertesting.2013.03.004

[31] Kilar V, Koren D, Bokan-Bosiljkov V. Evaluation of the performance of extruded polystyrene boards—Implications for their application in earthquake engineering. Polymer Testing. 2014;40:234–244. DOI: 10.1016/j.polymertesting.2014.09.013

[32] Maleki S, Ahmadi F. Using expanded polystyrene as a seismic energy dissipation device. Journal of Vibration and Control. 2011;17(10):1481–1497. DOI: 10.1177/1077546309357693

[33] Gibson LJ. Biomechanics of cellular solids. Journal of Biomechanics. 2005;38(3):377–399. DOI: 10.1016/j.jbiomech.2004.09.027

[34] Chen W, Hao H, Hughes D, Shi Y, Cui J, Li Z-X. Static and dynamic mechanical properties of expanded polystyrene. Materials & Design. 2015;69:170–180. DOI: 10.1016/j.matdes.2014.12.024

[35] CEN. European standard EN 12090:2013: Thermal insulating products for building applications - Determination of shear behaviour. Brussels, 2013.

[36] Vejelis S, Gnip I, Vaitkus S, Keršulis V. Shear strength and modulus of elasticity of expanded polystyrene (EPS). Medziagotyra. 2008;14(3):230–233.

[37] Calderini C, Abbati SD, Cotič P, Kržan M, Bosiljkov V. In-plane shear tests on masonry panels with plaster: correlation of structural damage and damage on artistic assets. Bulletin of Earthquake Engineering. 2015;13(1):237–256.
DOI: 10.1007/s10518-014-9632-y

[38] Azinović B, Kilar V, Koren D. Energy-efficient solution for the foundation of passive houses in earthquake-prone regions. Engineering Structures. 2016;112:133–145. DOI: 10.1016/j.engstruct.2016.01.015.

[39] Naeim F, Kelly JM. Design of seismic isolated structures: from theory to practice: John Wiley & Sons; 1999. 291 p.

[40] Hong WK, Kim HC. Performance of a multi-story structure with a resilient-friction base isolation system. Computers & Structures. 2004;82(27):2271–2283. DOI: 10.1016/j.compstruc.2004.06.002

[41] Panchal VR, Jangid RS. Seismic response of structures with variable friction pendulum system. Journal of Earthquake Engineering. 2009;13(2):193–216. DOI: 10.1080/13632460802597786

[42] Fadi F, Constantinou MC. Evaluation of simplified methods of analysis for structures with triple friction pendulum isolators. Earthquake Engineering & Structural Dynamics. 2010;39(1):5–22. DOI: 10.1002/eqe.930

[43] Koren D, Kilar V. The applicability of the N2 method to the estimation of torsional effects in asymmetric base-isolated buildings. Earthquake Engineering & Structural Dynamics. 2011;40(8):867–886. DOI: 10.1002/eqe.1064

[44] Becker TC, Mahin SA. Experimental and analytical study of the bi-directional behavior of the triple friction pendulum isolator. Earthquake Engineering & Structural Dynamics. 2012;41(3):355–373. DOI: 10.1002/eqe.1133

[45] Lu LY, Lee TY, Juang SY, Yeh SW. Polynomial friction pendulum isolators (PFPIs) for building floor isolation: An experimental and theoretical study. Engineering Structures. 2013;56:970–982. DOI: 10.1016/j.engstruct.2013.06.016

[46] Chung LL, Kao PS, Yang CY, Wu LY, Chen HM. Optimal frictional coefficient of structural isolation system. Journal of Vibration and Control. 2015;21(3):525–538. DOI: 10.1177/1077546313487938

[47] Polycarpou PC, Komodromos P. On poundings of a seismically isolated building with adjacent structures during strong earthquakes. Earthquake Engineering & Structural Dynamics. 2010;39(8):933–940. DOI: 10.1002/eqe.975

[48] Azinović B, Koren D, Kilar V. The seismic response of low-energy buildings founded on a thermal insulation layer – A parametric study. Engineering Structures. 2014;81:398–411. DOI: 10.1016/j.engstruct.2014.10.015

[49] Azinović B, Koren D, Kilar V. Principles of energy efficient construction and their influence on the seismic resistance of light-weight buildings. The Open Civil Engineering Journal. 2014;8:105–116. DOI: 10.2174/1874149501408010105

[50] CEN. Eurocode 8: Design of strucures for earthquake resistance—Part 1-1: General rules, seismic actions and rules for buildings. Brussels, 2005.

[51] Baker JW. Efficient analytical fragility function fitting using dynamic structural analysis. Earthquake Spectra. 2015;31(1):579–599. DOI: 10.1193/021113EQS025M

[52] Koren D, Kilar V. Seismic vulnerability of reinforced concrete building structures founded on an XPS layer. Accepted for publication in Earthquakes and Structures, An Int'l Journal. 2016.

[53] CSI. SAP2000 Structural and earthquake engineering software [Internet]. 2015. Available from: http://www.csiamerica.com/sap2000 [Accessed: 2015-12-3]